# Reevaluation of the direct sun measurements from the Brewer#001 for the retrieval of columnar $NO_2$ and AOD in the visible spectral range

Action number: CA21119

Applicant name: Aikaterini Anyfanti

Start and end date: 14/06/2026 to 27/06/2026

## 1. Introduction

While the Brewer spectrophotometer network is universally recognised for its high-quality ozone column measurements, its substantial potential for aerosol remote sensing remains largely unexploited. Most Brewer instruments measure aerosol optical depth (AOD) in the ultraviolet (UV-B) spectral region, complementing ground-based networks such as AERONET, which primarily operate in the visible and near-infrared spectrum. However, the MkIV Brewer subclass offers a unique and often overlooked capability: it can operate in the visible spectrum (425–435 nm), originally intended for nitrogen dioxide ($NO_2$) retrievals. This capability can also be used to estimate AOD in this critical wavelength range. Nevertheless, determining AOD in the visible spectrum using Brewer MkIV instruments is challenging due to the significant, structured spectral absorption of $NO_2$ in this wavelength range. Recent studies (Diémoz et al., 2021) have highlighted that this interference can introduce systematic biases in AOD retrievals if not properly accounted for. Fortunately, MkIV Brewers were specifically designed to operate in the visible domain, enabling the simultaneous retrieval of $NO_2$ vertical column densities through advanced algorithms. Accurate quantification of $NO_2$ from the same instrument enables direct correction of its optical depth contribution, providing a unique opportunity to derive high-quality, co-located visible-absorbance optical depth (VIS-AOD) measurements. These measurements complement UV-based AOD products from standard Brewer configurations and multi-wavelength observations from AERONET. This synergy is particularly valuable in urban and polluted environments, where anthropogenic aerosols and $NO_2$ emissions are closely correlated and co-vary in space and time. Exploiting the vast historical database of MkIV Brewers worldwide and implementing improved retrieval techniques (BNALG2 algorithm presented by Diémoz et al.) makes it feasible to reconstruct long-term, self-consistent time series of both $NO_2$ columns and VIS-AOD. This dual capability enhances the scientific utility of the existing Brewer network and offers a powerful, cost-effective tool for satellite validation, trend analysis and investigating aerosol-climate interactions. This addresses a critical gap in current ground-based observational capabilities. The steps that were followed to achieve the goals of the STSM, are described below.

## 2. Processing data from the Brewer #001

The Brewer spectrophotometer is a scanning ultraviolet (UV)-visible spectroradiometer that provides high-quality spectral measurements of direct solar irradiance. It is primarily used for total ozone observations, but can also be used to retrieve other atmospheric constituents, including nitrogen dioxide ($NO_2$) and aerosol optical depth (AOD). Solar radiation entering the instrument is spectrally dispersed by the monochromator and the transmitted irradiance is detected by a photomultiplier tube at specific wavelengths. These counts are then corrected for instrument-specific characteristics and calibrated to account for Brewer's operational performance and the effects of atmospheric absorption. This provides the basis for quantitative atmospheric retrievals. In this study, Brewer observations collected in Athens over a multi-year period were processed using a comprehensive retrieval methodology to derive $NO_2$ vertical column densities and AOD. This methodology involves characterizing the instrument's spectral response, evaluating operational wavelengths, determining effective absorption coefficients and retrieval weighting factors, assessing temperature-dependent effects and applying all necessary instrumental and atmospheric corrections for accurate $NO_2$ and aerosol retrievals. The individual processing steps are presented in the following sections.

### 2.1. Dispersion Test

To characterize the Brewer spectrophotometer and accurately map the micrometer steps to the wavelengths projected onto each slit, the dispersion test procedure was followed. This procedure is critical, as any misalignment in the monochromator calibration can introduce significant errors when retrieving atmospheric $NO_2$ and consequently when determining the aerosol optical depth (AOD). This is due to the overlapping spectral features and the need for accurate wavelength registration in aerosol retrievals. Rather than using the dispersion coefficients from the ultraviolet (UV) region, this study performed an independent dispersion test specifically for the visible spectrum. This followed the improved methodology proposed in the literature (Gröbner et al., 1998) and applied the new algorithm developed within the framework of this thesis. The data used in the present analysis were derived from the calibration files of Brewer #001, which were obtained during the instrument's calibration procedure in 2019. Processing these files determined the exact operating wavelengths and the resolution of each slit, assuming a linear variation of the resolution with respect to the micrometer step, in accordance with the literature.

*Figure 1* shows an example of the dispersion test results. The left panel displays a scan of an emission line for slit 3, showing the forward and backward scans alongside the isosceles triangle fit used to determine the line center. The right panel shows the resolution (FWHM) of the same slit as a function of the micrometer step, confirming the linear variation of the resolution with respect to the grating position.

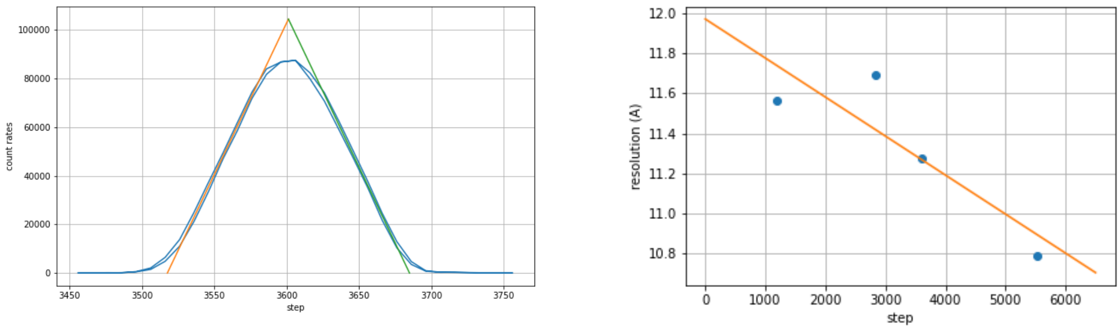


*Figure 1 : Results from the dispersion test for slit 3. Left panel: scan of an emission line showing the forward and backward measurements along with the isosceles triangle fit used to determine the line center. Right panel: resolution (FWHM) of the slit as a function of the micrometer step, illustrating the linear variation of the resolution with respect to the grating position.*

Following the dispersion test procedure, the operational wavelengths for the $NO_2$ measurements were determined as follows: First, a linear fit was performed for each slit, using the UV wavelengths obtained from the $O_3$ dispersion test as a function of the motor steps. These wavelengths were then multiplied by a factor of 1.5 to account for the different diffraction order used in visible mode ($NO_2$) compared to UV mode ($O_3$). A vertical line was then drawn at step 980, corresponding to the operational step for $NO_2$ as determined by this specific dispersion test. The intersection points of this vertical line with the fitted curves for each slit yielded the operational wavelengths for $NO_2$. Figure 2 shows the resulting dispersion curves for all six slits, while Table 1 lists the derived operational wavelengths for each slit.

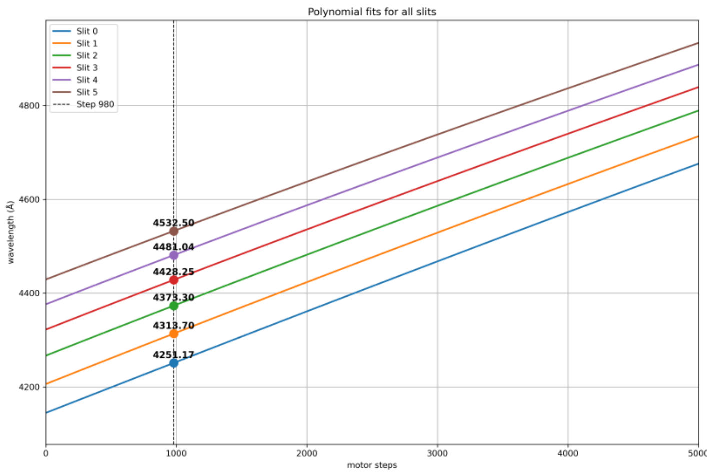


*Figure 2 : Dispersion curves for all six slits as a function of motor steps. The vertical dashed line at step 980 marks the operational step for $NO_2$, and the intersection points yield the operational wavelengths for each slit (listed in Table 1).*

*Table 1 : Operational wavelengths and resolutions (in nm) for each slit at step 980 for Brewer #001, as derived from the dispersion test for $NO_2$ measurements.*

| Slit | Wavelength (nm) | Resolution (nm) |
|---|---|---|
| **0** | 425.1 | 0.61 |
| **1** | 431.4 | 0.85 |
| **2** | 437.3 | 0.84 |
| **3** | 442.8 | 0.88 |
| **4** | 448.1 | 0.89 |
| **5** | 453.2 | 0.86 |

## 2.2. Weightings coefficients - $NO_2$ cross sections

The weightings ($\gamma_i$) are coefficients used in the linear combination of the measured irradiances from different slits. They serve to isolate the $NO_2$ signal by cancelling out contributions from other atmospheric species and scattering processes (Diémoz, 2014). To achieve this, the weightings must satisfy specific orthogonally conditions with respect to the spectral signatures of Rayleigh scattering, ozone absorption, aerosol extinction and wavelength-independent factors (Diémoz et al., 2021). Satisfying these conditions enables the linear combination to eliminate interfering signals and isolate the $NO_2$ contribution. These conditions are shown below:

$\Sigma\, \gamma_i = 0$ (removes spectrally-flat factors)

$\Sigma\, \gamma_i \cdot \tau_{R_i} = 0$ (removes Rayleigh scattering)

$\Sigma\, \gamma_i \cdot \lambda_i^{-1} = 0$ (removes aerosol Mie scattering)

$\Sigma\, \gamma_i \cdot \partial(\log I)/\partial\lambda|_i = 0$ (minimizes sensitivity to wavelength shifts) (2.2.1)

By satisfying these conditions, the linear combination eliminates the interfering signals and isolates the $NO_2$ contribution.

The weightings for Brewer #001 were derived based on the 2019 calibration files and the dispersion test results, following the BNALG2 methodology (Diémoz., 2014). The total direct solar spectrum was calculated using the Beer–Lambert law, taking into account the contributions of Rayleigh scattering, ozone, aerosols and $NO_2$ at a solar zenith angle of 60°. Brewer's slit functions were then applied to determine the intensities measured by the instrument at each slit. These weightings were obtained by solving the system of orthogonally equations (Equation 2.2.1), with one degree of freedom left to maximize the signal-to-noise ratio (SNR) and minimize interference from unaccounted species. The resulting weightings for Brewer #001 are presented in Table 2.

*Table 2 : Weightings ($\gamma_i$) derived for Brewer #001 following the BNALG2 methodology, based on the 2019 calibration and dispersion test results.*

| Slit | Weighting |
|---|---|
| **0** | 0.052138 |
| **1** | 0.062605 |
| **2** | -0.268481 |
| **3** | -0.271192 |
| **4** | 0.827872 |
| **5** | -0.402942 |

The weightings are used in the Brewer to calculate the $NO_2$ vertical column density (VCD):

$$X_{NO_2} = \frac{\sum \gamma_i \cdot \log(I_{0i}) - \sum \gamma_i \cdot \log(I_i)}{\mu_{NO_2} \cdot \sum \gamma_i \cdot \sigma_{NO_{2i}}} \qquad (2.2.2)$$

where log $I_{0i}$ and log $I_i$ are the logarithmic extraterrestrial and measured intensities at each slit, respectively, $\mu_{NO_2}$ is the $NO_2$ air mass factor, and $\sigma_{NO_{2i}}$ is the $NO_2$ absorption cross section.

The differential $NO_2$ absorption coefficient was then calculated as the linear combination of the $NO_2$ absorption cross sections and the derived weightings:

$$\boldsymbol{\sum \gamma_i \cdot \sigma_{NO_{2i}} = 2.21663 \cdot 10^{-19}\ cm^2 \cdot molec^{-1}}$$

## 2.3. Effect of atmospheric interferences ($O_3$, $O_2$–$O_2$) on $NO_2$ retrievals

Atmospheric absorbers such as $O_3$ (ozone) and $O_4$ (oxygen dimer) can significantly interfere with $NO_2$ retrievals because their absorption features may overlap with those of $NO_2$ within the visible spectral range. If these interferences are not properly accounted for, they can introduce systematic errors in the retrieved $NO_2$ slant columns, affecting calculations of aerosol AOD. To quantify these effects, we examined $O_3$ and $O_4$ interferences. For $O_4$, we calculated the total absorption of $O_4$ over Athens as a function of wavelength in order to quantify its subsequent impact on $NO_2$ and, consequently, on aerosol AOD. We then computed the effective $O_4$ absorption that the instrument would actually measure for each of the six instrument slits. By comparing this $O_4$ absorption spectrum with that of $NO_2$, we estimated the error that would arise if $O_4$ were ignored which amounted to **0.0418 DU**. Similarly, we investigated ozone's interference with $NO_2$ and found the ratio ($x_s$_ratio) between the ozone differential absorption coefficient and that of $NO_2$. The resulting error due to unaccounted ozone in $NO_2$ retrievals is given by:

$$\frac{O_3 \text{ slant column } \cdot x_s \text{ ratio}}{\text{airmass}} \qquad (2.3.1)$$

Where **$x_s$ ratio = - 5.904e-05** and **$O_{3eff}$= -0.0177 DU**.

## 2.4. Effect of the neutral density filters on $NO_2$ retrievals

Neutral density filters are used to control the intensity of the light collected by the instrument, and they should attenuate irradiance at all wavelengths by the same amount. However, previous studies (Savastiouk, 2005) have shown that this assumption is not strictly valid, as real filters exhibit wavelength-dependent transmission features that can distort the measured spectra. In our instrument, five neutral density filters are used to regulate the signal to the desired levels at which the instrument's response is linear. The attenuation of these ND filters is measured using an internal lamp, and these measurements were analyzed throughout the instrument's operating period. Such non-neutral behavior can introduce systematic errors in the retrieved $NO_2$ slant columns, as the filter-induced structures may be misinterpreted as $NO_2$ absorption or affect the accuracy of the spectral fitting process. Consequently, any error in $NO_2$ retrieval is propagated directly to aerosol optical depth (AOD) retrieval in the visible spectral range, since $NO_2$ is one of the key trace gases that must be accurately subtracted before deriving aerosol properties.

To assess the attenuation of each filter, we used JF files generated by jf.rtn, a routine developed by Henri Diemoz (2014) that measures attenuation only at the grating position typically employed in $N_2$ mode. In practice, the Brewer #001 observes the light source (lamp) through different filters. For each filter, we recorded the measurement time, the filter position (filterpos), the number of counts from the six slits, the dead time and the number of cycles. We applied corrections for counts per second and dead time and performed interpolation to enable comparison of the filters at the same time reference. This enabled us to determine the attenuation of each filter for every slit. Finally, we quantified the effect of each filter on the final $NO_2$ retrieval on Table 3.

*Table 3 : Attenuation factors of the five neutral density filters (same for all slits), derived from internal lamp measurements.*

| Filter | Attenuation of each filter |
|---|---|
| 1 | -3.238e-03 |
| 2 | -4.198e-03 |
| 3 | -1.644e-02 |
| 4 | -1.655e-02 |
| 5 | -1.034e-01 |

## 2.5. Effect of temperature

Temperature is another critical factor that can affect retrieval accuracy. Variations in temperature can affect the sensitivity of the photomultiplier tube (PMT), the dark current and potentially the filter transmission characteristics, thereby influencing the instrument's response. Temperature fluctuations can also cause slight shifts in wavelength calibration and affect the stability of the measured counts. Although temperature does not significantly impact $NO_2$ retrieval itself, it notably affects aerosol optical depth (AOD) calculations. This is because temperature-induced variations in the instrument's response can introduce errors in the spectral calibration and measured irradiance, both of which are critical for accurately determining the AOD in the visible range (Diemoz et al, 2016).

To assess the significance of these temperature-induced effects and examine their temporal stability, the temperature sensitivity of the Brewer instrument was investigated throughout the study period using Standard Lamp (SL) measurements. For each 10-day period, the normalized Standard Lamp signal was correlated with the instrument temperature, and the corresponding temperature sensitivity (slope) was calculated for each wavelength. The mean slope and its temporal variability were then evaluated. In Figure 3 are presented the results for 2021 as a representative example.

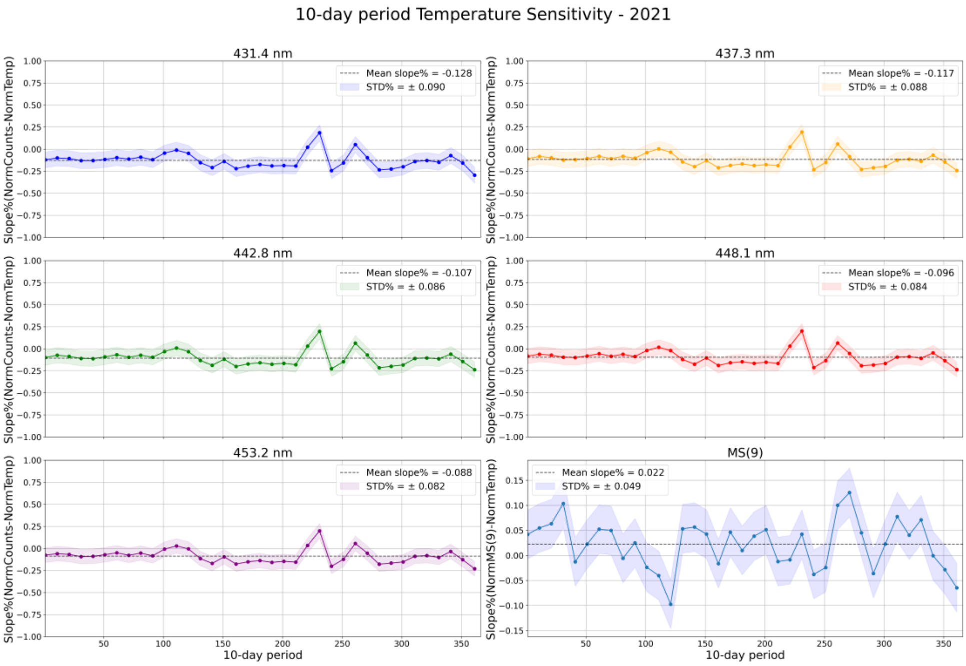


*Figure 3 : Temperature sensitivity of the normalized Brewer Standard Lamp (SL) signal for the visible wavelengths and MS(9) during 2022. The dashed line indicates the annual mean slope, while the shaded area represents ±1 standard deviation.*

Figure 4 illustrates the dependence of the Brewer Standard Lamp F-ratio on the instrument temperature for March–May 2021. The Standard Lamp measurements were first corrected for counts per second and dead-time effects before calculating the F-ratio. For the calculation of the F-Ratio, the weightings presented in Table **2** were used. A linear regression was then applied, with the resulting slope (**0.0058 DU/°C**) representing the temperature sensitivity of the instrument during this period. The positive slope indicates a gradual increase of the F-ratio with increasing temperature.

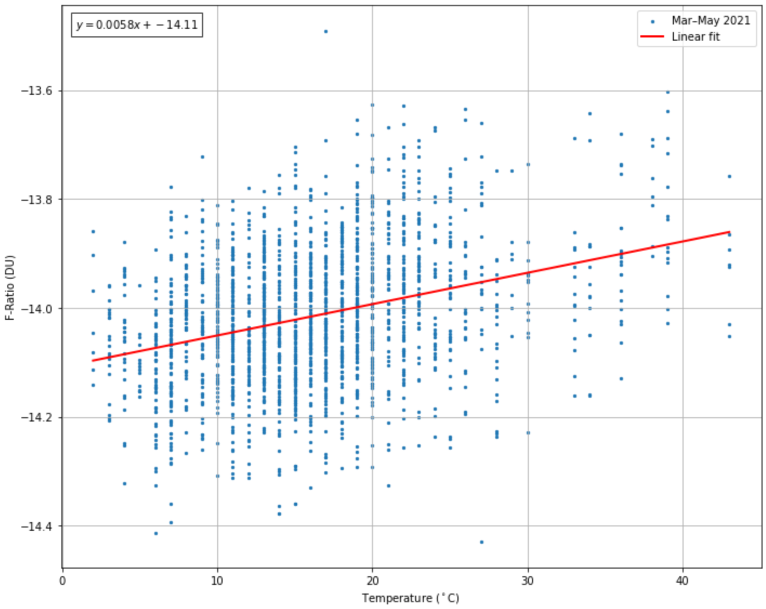


*Figure 4 : Temperature dependence of Brewer #001 for March-May 2021*

## 2.6. Calculation of the Extraterrestrial Constant (ETC)

To estimate the extraterrestrial coefficient, we used the n2ds data from the Brewer B-files. The raw counts were first converted to counts per second and corrected for dead time as well as Rayleigh scattering effects. For each wavelength, we then computed the $F_i$ (Equation 2.5.1) values using the corrected signal, the atmospheric pressure measured during the corresponding period, and the air mass factor (AMF) associated with each individual measurement.

$$F_i = \log(\text{correced signal}) * 10^4 + \frac{\text{AMF} * \text{tau}_{\text{Rayleigh}} * \text{pressure} * 10^4}{1013.25} \qquad (2.5.1)$$

Then, using again the weightings from Table 2 and $NO_2$ absorption cross sections, we computed the $NO_2$ double ratio as described in Equation 2.5.2 expressed in DU (DU = Dobson Units).

$$MS9 = \frac{\sum_i \gamma_i \cdot F_i}{\log e \cdot 10^4 \cdot 2.216 \cdot 10^{-19} \cdot 2.687 \cdot 10^{19}} \cdot 10^3 \qquad (2.5.2)$$

Then, we computed the ETC again, expressed in Dobson Units (DU), using Equation 2.5.3.

$$ETC = MS9 + AMF \cdot Backround_{NO2} \qquad (2.5.3)$$

The background $NO_2$ is calculated using the "minimum-amount Langley extrapolation" (MLE) (Diemoz et al, 2021) method, for which a value of 0.12 DU was obtained for Athens (Diemoz, 2014).
Thus, the ETC for the last decade was derived after first being smoothed on a quarterly basis. The results are shown in Figure 5.

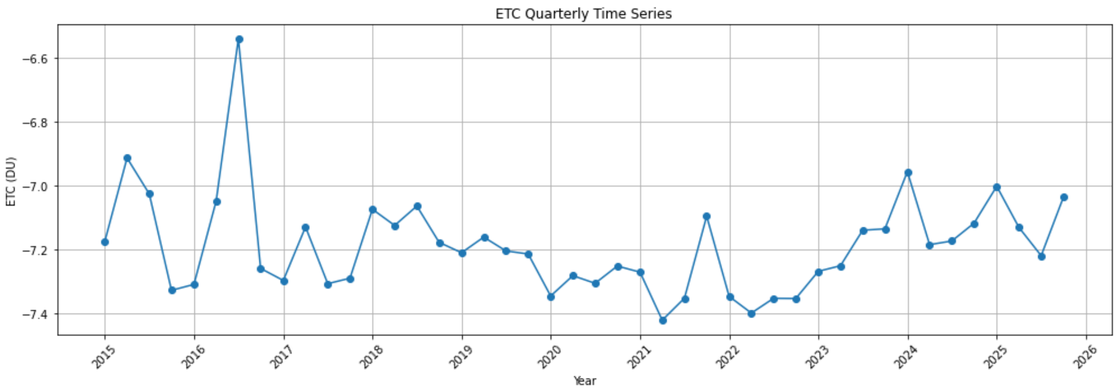


*Figure 5 : Quarterly smoothed ETC (DU) time series over the last decade (2015–2025).*

### 2.7. $NO_2$ retrievals

After deriving the extraterrestrial coefficient, $NO_2$ concentrations for the past decade were retrieved in Dobson Units (DU) in Figure ***6***. The values presented here are preliminary and have not yet been corrected for $O_3$ and $O_4$ absorption effects or for instrument filter influences. These corrections will be incorporated in the final $NO_2$ retrieval algorithm.

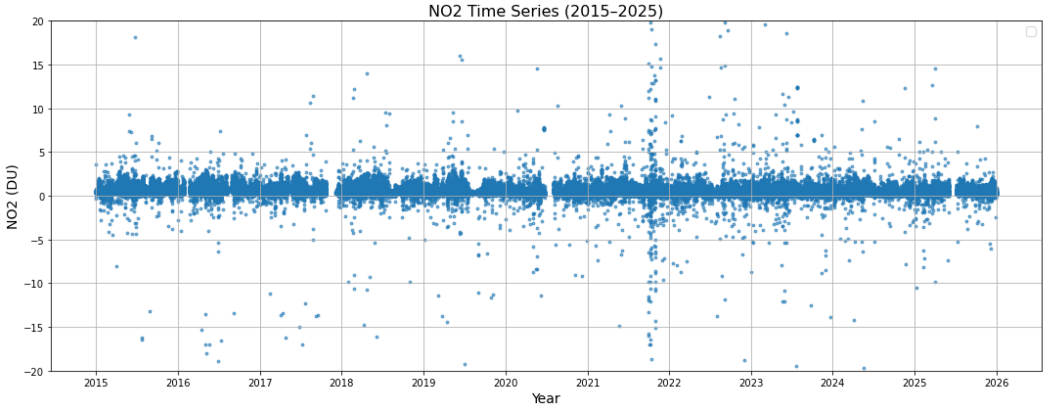


*Figure 6 : NO2 retrievals time series over the last decade (2015-2025) in Athens from Brewer #001 measurements*

## 3. Summary and future actions

The STSM successfully achieved its main objective of enabling the reconstruction and comprehensive understanding of the visible retrieval methodology developed by the host institution for deriving nitrogen dioxide ($NO_2$) and aerosol optical depth (AOD) from MKIV Brewer direct sun measurements. The complete processing chain was studied in detail, including determining the operating wavelengths, calculating effective $NO_2$ absorption cross-sections and differential absorption coefficients, estimating extraterrestrial constants (ETCs) and implementing the required corrections for $O_4$ and $O_3$ absorption, as well as the spectral response of the Brewer neutral density filters. Additionally, the temperature dependence of the instrument was investigated using internal standard lamp measurements to evaluate its impact on the stability of visible observations and AOD retrievals. The reconstruction and implementation of the retrieval algorithm successfully established a solid basis for the consistent reprocessing of the historical Brewer #001 dataset, as well as for future scientific analyses of long-term atmospheric composition over Athens.

The work carried out during the STSM provides the foundation for several follow-up activities. The next step will be to process the complete Brewer#001 historical time series to retrieve continuous $NO_2$ and AOD records. These products will then be validated by comparing them with independent ground-based measurements, such as those from the Pandora instrument operating in Athens. Finally, the resulting long-term datasets will be used to perform a climatological analysis of $NO_2$ and AOD over Athens, investigating their temporal variability, long-term trends and potential links with changes in emissions and atmospheric processes.

## References


Barton, D.V. (2007). The measurement of $NO_2$ using Brewer spectrophotometers. Available:https://www.collectionscanada.gc.ca/obj/thesescanada/vol2/002/MR29273.PDF?is_thesis=1&oclc_number=456827230.

Henri Diémoz, Anna Maria Siani, Stefano Casadio, Anna Maria Iannarelli, Casale, G., Vladimir Savastiouk, Cede, A., Tiefengraber, M. and Moritz Müller (2021). Advanced NO<sub>2</sub> retrieval technique for the Brewer spectrophotometer applied to the 20-year record in Rome, Italy. *Earth System Science Data*, 13(10), pp.4929–4950. doi:https://doi.org/10.5194/essd-13-4929-2021.

H. Diémoz, Siani, A.M., A. Redondas, V. Savastiouk, McElroy, C.T., M. Navarro-Comas and Hase, F. (2014). Improved retrieval of nitrogen dioxide (NO<sub>2</sub>) column densities by means of MKIV Brewer spectrophotometers. Atmospheric measurement techniques, 7(11), pp.4009–4022. doi:https://doi.org/10.5194/amt-7-4009-2014.

Henri Diémoz, Kostas Eleftheratos, Stelios Kazadzis, Vassilis Amiridis and Zerefos, C.S. (2016). Retrieval of aerosol optical depth in the visible range with a Brewer spectrophotometer in Athens. *Atmospheric measurement techniques*, 9(4), pp.1871–1888. doi:https://doi.org/10.5194/amt-9-1871-2016.

Henri Diémoz : Improvements to the nitrogen dioxide observations by means of the MKIV Brewer spectrophotometer, Ph.D. thesis, 2014.

Savastiouk, V.: Improvements to the direct-sun ozone observations taken with the Brewer spectrophotometer, Ph.D. thesis, 2005.